Spin dynamics of the charge-transfer phase transition of an iron mixed-valence complex observed using muon spin relaxation spectroscopy

N. Kida,[1] M. Enomoto,[1] I. Watanabe,[2] T. Suzuki,[2] and N. Kojima[1]
[1]*Graduate School of Arts and Sciences, The University of Tokyo, 3-8-1 Komaba, Meguro-ku, Tokyo 153-8902, Japan*
[2]*Advanced Meson Science Laboratory, RIKEN Nishina Center, 2-1 Hirosawa, Wako, Saitama 351-0198, Japan*
(Received 1 December 2007; revised manuscript received 9 April 2008; published 25 April 2008)

Muon spin relaxation was performed to investigate the dynamic properties of electrons in the iron mixed-valence complex $(n\text{-}C_3H_7)_4N[Fe^{II}Fe^{III}(dto)_3]$ $(dto=C_2O_2S_2)$, which shows a charge-transfer phase transition around 120 K and a ferromagnetic transition at 7 K. The dynamic muon spin depolarization rate for $(n\text{-}C_3H_7)_4N[Fe^{II}Fe^{III}(dto)_3]$ in zero field exhibits an anomalous enhancement with thermal hysteresis between 60 and 140 K, which is due to the charge-transfer phase transition. The nature of the charge transfer is the oscillation of electrons between Fe^{II} and Fe^{III} sites, producing a dynamically fluctuating internal field at the muon site with a frequency of about 0.1 MHz.

DOI: 10.1103/PhysRevB.77.144427 PACS number(s): 75.50.Xx, 75.40.Gb, 76.75.+i

I. INTRODUCTION

A valence instability or bistability in solid state materials leads to an intramolecular and intermolecular electron transfer when external stimuli, such as temperature change, pressure, or light irradiation, are applied, which plays a key role in producing novel electronic, magnetic, and/or optical functionalities. A typical example is the first order phase transition called charge transfer phase transition (CTPT). The CTPT is a new type of conjugated phenomenon coupled with spins and charges wherein a thermally induced metal-to-metal or metal-to-ligand electron transfer occurs to minimize the free energy in the whole system.[1] As a result of electron transfer, the spin degeneracy changes without spin transition, which is quite different from a classical spin crossover. This spin-entropy effect has an important role in the driving force of CTPT. Since the discovery in the iron mixed-valence complex $(n\text{-}C_3H_7)_4N[Fe^{II}Fe^{III}(dto)_3]$ $(dto=C_2O_2S_2)$,[2] the CTPT has been observed in several transition metal complexes[3–6] by magnetic susceptibility measurements,[2–6] calorimetry measurements,[1,4] vibrational spectroscopy,[4,5] and Mössbauer spectroscopy.[2,6] In the case of $(n\text{-}C_3H_7)_4N[Fe^{II}Fe^{III}(dto)_3]$ (hereafter denoted as $n=3$), Fe^{II} and Fe^{III} are alternately linked by dithiooxalato molecules, which forms a two-dimensional honeycomb network structure.[7] In this compound, the thermally induced charge-transfer between Fe^{II} and Fe^{III} sites reversibly occurs around 120 K. Consequently, the spin configuration changes between $Fe^{II}(S=2)-Fe^{III}(S=1/2)$ [high-temperature phase (HTP)] and $Fe^{II}(S=0)-Fe^{III}(S=5/2)$ [low-temperature phase (LTP)]. With a further decrease in temperature below 7 K, Fe spins have been found to be in a ferromagnetically ordered state. In the case of $(n\text{-}C_5H_{11})_4N[Fe^{II}Fe^{III}(dto)_3]$ (hereafter denoted as $n=5$), the CTPT does not occur and the spin configuration of $Fe^{II}(S=2)-Fe^{III}(S=1/2)$ corresponding to the HTP in $n=3$ undergoes a ferromagnetic transition at 20 K.[8,9]

Although an understanding of the mechanism of electron transfer in such materials is of great importance, the nature of the CTPT, dynamic properties of electron transfer in particular, has not been fully understood. One key question about the CTPT is whether electrons are statically localized or dynamically fluctuated between Fe sites under thermal equilibrium condition. It is known that ^{57}Fe Mössbauer spectroscopy provides us with not only information about the valence state of iron atoms but also their spin configurations. Dynamic features of the mixed-valence states are also detectable through the line-broadening Mössbauer spectra when the valence state is fluctuating over the Mössbauer time scale.[10–13] In connection with ^{57}Fe Mössbauer spectroscopy, we measured the ^{57}Fe Mössbauer spectra of $n=3$ and observed the CTPT.[2] Here, we show more detailed spectra of $n=3$ at several temperatures around the CTPT in Fig. 1. At 130 K, only two quadrupole-split doublets corresponding to the HTP are observed. As the temperature decreases, the intensity of the HTP doublets decreases and two new quadrupole-split doublets corresponding to the LTP appear. Judging from the analysis of the line profile around 120 K, the coexistence of the HTP and LTP in the vicinity of the CTPT has been confirmed and both of these phases are clearly distinguishable. This result indicates that the valence state of Fe is static at least on the Mössbauer time scale during the CTPT. Therefore, the dynamics of the electron transfer cannot be directly probed by Mössbauer spectroscopy. It is thus important for the investigation of CTPT to explore another experimental method that provides the dynamic information at a microlevel.

In this paper, we report the results of zero-field (ZF) and longitudinal-field (LF) muon spin relaxation (μSR) measurements for $n=3$ and 5 to investigate the dynamics of the electron transfer between Fe^{II} and Fe^{III}, which is accompanied by the CTPT. Since the μSR technique is based on the observation of the evolution with time of the direction of the muon spin in the magnetic field at the muon site in the sample, it is a very useful technique that probes the magnitude, distribution, and dynamics of the internal fields. It is a versatile technique that has been applied to inorganic and organic magnets, superconductors, and radicals. Moreover, since μSR has a wider characteristic time window (typically from 10^{-5} to 10^{-11} s) than the ^{57}Fe Mössbauer spectroscopy (10^{-7} s), μSR can be a more sensitive microscopic probe to sense the dynamics of CTPT within a wider frequency range rather than Mössbauer spectroscopy.

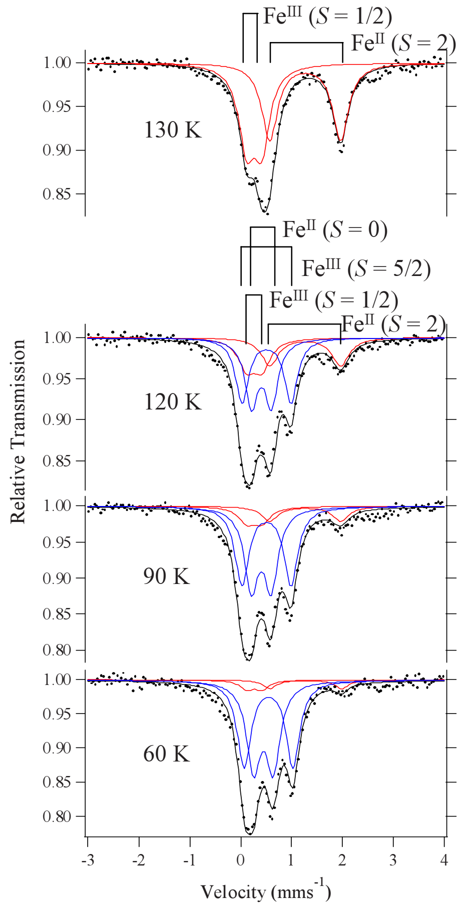

FIG. 1. (Color online) ^{57}Fe Mössbauer spectra of $(n\text{-}C_3H_7)_4N[Fe^{II}Fe^{III}(dto)_3]$ at 130, 120, 90, and 60 K. The sample was cooled from room temperature.

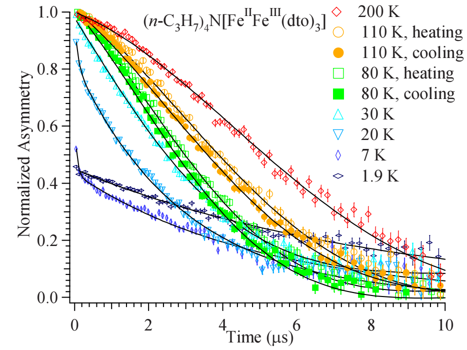

FIG. 2. (Color online) Zero-field μSR time spectra of $(n\text{-}C_3H_7)_4N[Fe^{II}Fe^{III}(dto)_3]$. The solid lines show the best fit of Eq. (1). The spectra at 80 and 110 K show both the heating and the cooling processes.

II. EXPERIMENT

Powder samples of $n=3$ and 5 were prepared in a similar way to that reported in a previous paper.[9] A μSR experiment was performed at the RIKEN-RAL Muon Facility in the United Kingdom by using a pulsed positive surface-muon beam.[14] The time dependence of the asymmetry parameter of muon spin polarization (μSR time spectrum) was measured in ZF and a LF. The asymmetry parameter is defined as $A(t)=[F(t)-\alpha B(t)]/[F(t)+\alpha B(t)]$, where $F(t)$ and $B(t)$ are the total muon events of the forward and backward counters aligned in the beam line, respectively. The initial asymmetry, $A(0)$, is defined as the asymmetry at $t=0$. α is a calibration factor that reflects the relative counting efficiencies between the forward and backward counters. The initial muon spin polarization is in parallel with the beam line and the direction of the LF is parallel to the internal muon spin polarization.

III. RESULTS AND DISCUSSION

A. Zero-field muon spin relaxation

Figure 2 shows the ZF-μSR time spectra of $n=3$ between 1.9 and 200 K. A Gaussian-type depolarization behavior of the time spectrum is observed at 200 K. The time spectrum changes to an exponential type with decreasing temperature below 30 K, and a loss of the initial asymmetry is observed below 20 K. Within a time region longer than 1 μs, the time spectrum slightly recovers with decreasing temperature down to 1.9 K. This series of behaviors is a sign of the appearance of the ferromagnetically ordered state ($T_C=7$ K). Furthermore, thermal hysteresis is observed around 120 K, at which the CTPT occurs. The time spectra obtained at 80 and 110 K in the cooling process are always located below those obtained at the same temperatures in the heating process. This means that the muon spin depolarizes faster in the cooling process than in the heating process. The tendency of hysteresis in the temperature dependence of the muon spin depolarization behavior around 80 K is consistent with that observed in our previous magnetic susceptibility measurement.[2]

To parametrize the time spectrum, the following function with two components was used to analyze all of the time spectra:

$$A_0 G_Z(\Delta, H_{LF}, t)\exp(-\lambda_0 t) + A_1 \exp(-\lambda_1 t), \qquad (1)$$

where A_0 and A_1 are the initial asymmetries of the slow and fast relaxation components and λ_0 and λ_1 are the respective muon spin depolarization rates. $G_Z(\Delta, H_{LF}, t)$ is the static Kubo–Toyabe function.[15] Δ/γ_μ is the distribution width of the nuclear-dipole fields at the muon sites, and γ_μ is the gyromagnetic ratio of muon spin ($2\pi\times 13.55$ MHz/kG). The H_{LF} is the LF. In the case of ZF, we set H_{LF} to zero. The first term was applied to the time spectra obtained above 30 K by substituting $A_1=0$. In this case, λ_0 describes the effects of dynamically fluctuating internal fields at the muon site. The time spectrum does not exhibit a Gaussian shape below 30 K, indicating that the effect of nuclear dipole fields is masked by strong internal fields related to the appearance of the ferromagnetically ordered state. In this case, the value of Δ is effectively set as zero. Then, λ_0 represents the long-time muon spin depolarization behavior observed at times longer than 10 μs and describes the effect of slowly fluctuating internal fields at the muon site. On the other hand, the second term represents the fast depolarization behavior within 1 μs, which reflects the strong effect related to the ferromagneti-

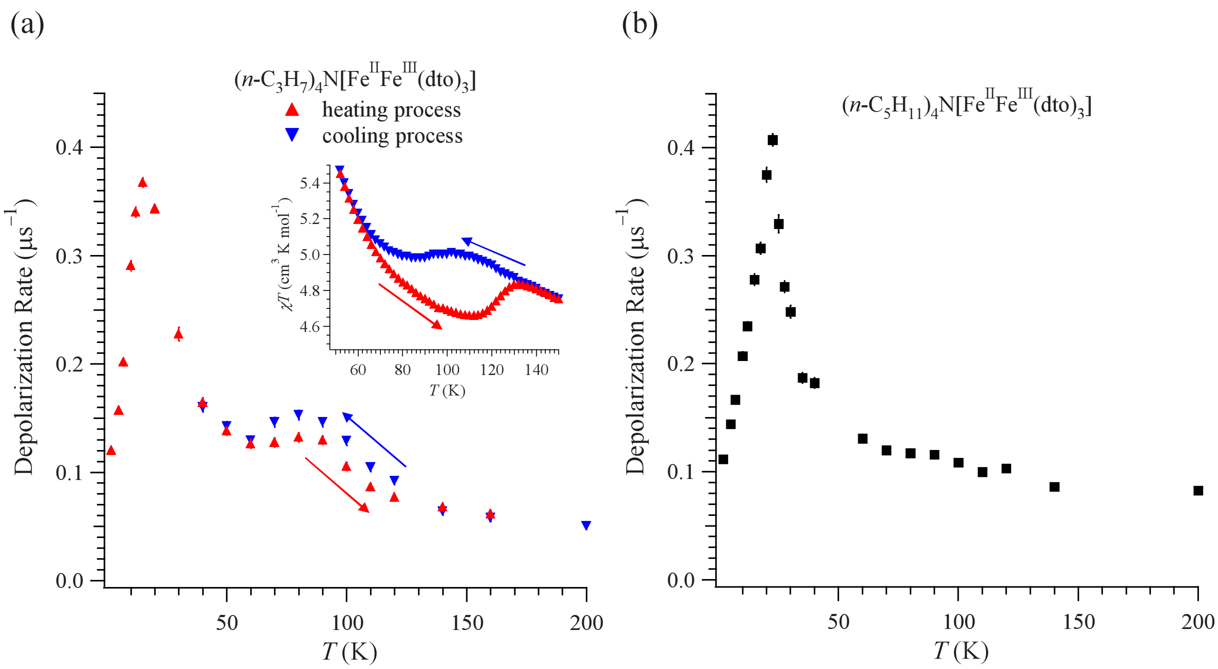

FIG. 3. (Color online) (a) Temperature dependence of the dynamic muon spin depolarization rate λ_0 for $(n\text{-}C_3H_7)_4N[Fe^{II}Fe^{III}(dto)_3]$ in the cooling and heating processes. The inset shows the temperature dependence of the molar magnetic susceptibility for $(n\text{-}C_3H_7)_4N[Fe^{II}Fe^{III}(dto)_3]$. ← and → denote the heating and cooling processes, respectively. (b) Temperature dependences of λ_0 for $(n\text{-}C_5H_{11})_4N[Fe^{II}Fe^{III}(dto)_3]$.

cally ordered state. The solid lines in Fig. 2 are the best-fit results of Eq. (1).

Figure 3(a) displays the temperature dependence of λ_0 for $n=3$. λ_0 exhibits a peak at 15 K. Since the ferromagnetic transition temperature has been estimated at 7 K from the susceptibility measurement, the enhancement of λ_0 above 15 K is due to the critical slowing down of the fluctuations of Fe spins toward the ferromagnetic transition.[16] Moreover, an anomalous enhancement with thermal hysteresis of λ_0 was observed between 60 and 140 K. Because no thermal hysteresis was observed in Δ, the thermal hysteresis of λ_0 is caused by the changes in the dynamic properties of electrons. The range of temperatures wherein the anomalous enhancement of λ_0 was observed is well matched with the temperature range wherein the CTPT appears [see the inset of Fig. 3(a)]. We also measured the ZF-μSR of $n=5$ for comparison because both the thermal hysteresis of the susceptibility and the CTPT were not observed.[6,7] The time spectra for $n=5$ were analyzed in the same way as for $n=3$ by using Eq. (1). Figure 3(b) displays the temperature dependence of λ_0 for $n=5$. λ_0 increases with decreasing temperature below 200 K. Values of λ_0 for $n=5$ are similar to those for $n=3$ at the measuring temperatures except for the temperature region wherein the CTPT occurs. This fact means that depolarization mechanism of the muon spin in the case of $n=5$ is similar to that of $n=3$ except for the effect of CTPT. A strong enhancement was observed around 22 K, which is due to the critical slowing down of Fe spins toward the ferromagnetically ordered state and was observed as well in the case of $n=3$. Since the anomalous enhancement of λ_0 with thermal hysteresis around 80 K is observed only for $n=3$, it is concluded that it originates from the CTPT. Taking into account that the CTPT is accompanied by the electron transfer and the HTP state is mixed with the LTP state around 80 K in the case of $n=3$, it can be concluded that the motion of electrons between the Fe^{II} and Fe^{III} sites induces fluctuating internal fields at the muon site enhancing λ_0. Therefore, the oscillation of electrons between Fe spins is the nature of CTPT.

B. Longitudinal-field muon spin relaxation

To obtain more detailed information on the dynamic properties of the electron transfer, LF-μSR was performed at 60, 80, and 110 K in the cooling process for both $n=3$ and 5. Figure 4 shows the LF dependence of the time spectrum at 80 K. The depolarized time spectrum recovers with increas-

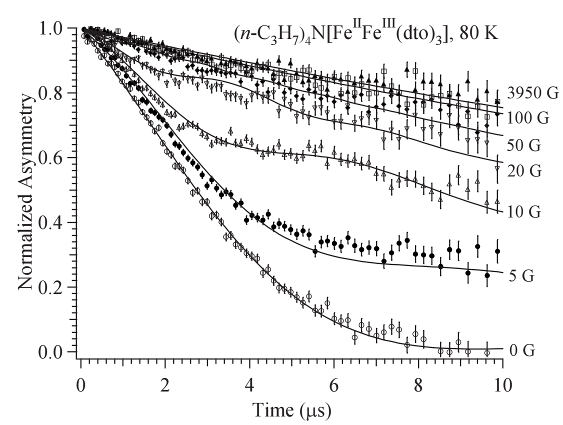

FIG. 4. Longitudinal-field dependence of the time spectra of $(n\text{-}C_3H_7)_4N[Fe^{II}Fe^{III}(dto)_3]$ at 80 K in the cooling process. The solid lines show the best fit of Eq. (1).

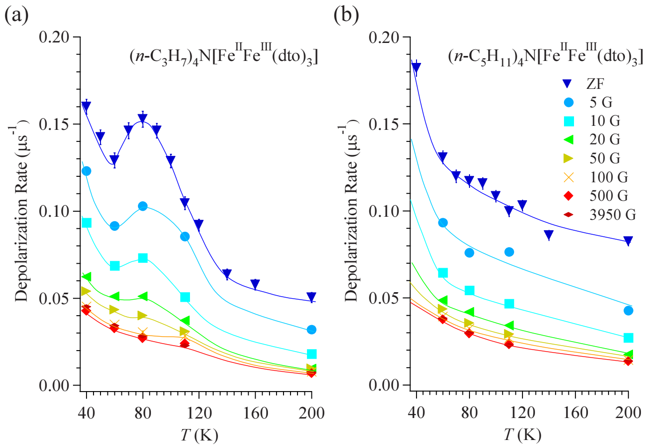

FIG. 5. (Color online) (a) Temperature and longitudinal-field dependence of the dynamic muon spin depolarization rate, λ_0, for $(n\text{-}C_3H_7)_4N[Fe^{II}Fe^{III}(dto)_3]$. (b) Temperature and longitudinal-field dependence of λ_0 for $(n\text{-}C_5H_{11})_4N[Fe^{II}Fe^{III}(dto)_3]$. The solid lines are guides for the eye.

ing LF up to about 100 G, showing the typical decoupling behavior of the nuclear dipole fields by the application of a LF. Above 100 G, the time spectrum changes little up to the maximum field of about 4 kG and the slow depolarization behavior remains even at 4 kG. The time spectra were analyzed by using Eq. (1) and fixing A_1 as zero. Both A_0 and Δ were set as constant values and were obtained from the fitting of the time spectrum at the same temperature in ZF. The solid lines in Fig. 4 show the best-fit results.

Figures 5(a) and 5(b) display the temperature and LF dependences of λ_0 for $n=3$ and 5, respectively. In the case of $n=3$, the peak around 80 K disappears with increasing LF. λ_0 for both $n=3$ and 5 decreases with increasing LF up to about 100 G and becomes constant above 100 G with a value of about 0.03 μs^{-1} each. The constant values increase with decreasing temperature. There seems to be two components in the LF dependence of λ_0. One is easily suppressed by a weak LF of about 100 G and shows a convex shape in its LF dependence (the weak component), and the other is independent of the LF up to 4 kG (the strong component). The weak component means that there is a small and slowly fluctuating internal field at the muon site, which is easily masked by a small LF. Although the origin of the weak component is not clear at the moment, it would be suggested to be due to the fluctuating component of nuclear dipoles as was observed in MnSi.[17] As for the strong component, considering that the value of the strong component increases with decreasing temperature and similar values of λ_0 are observed in both cases of $n=3$ and 5 at the same temperature, it is suggested that the strong component originates from the dipole field of dynamically fluctuating Fe spins. Then, the electron transfer due to the CTPT has an additional effect on the weak component of the muon spin depolarization. This means that electrons oscillating between the Fe^{II} and Fe^{III} sites make dynamically fluctuating internal fields at the muon site. The additional depolarization rate due to the CTPT (λ_{CT}) is extracted as follows:

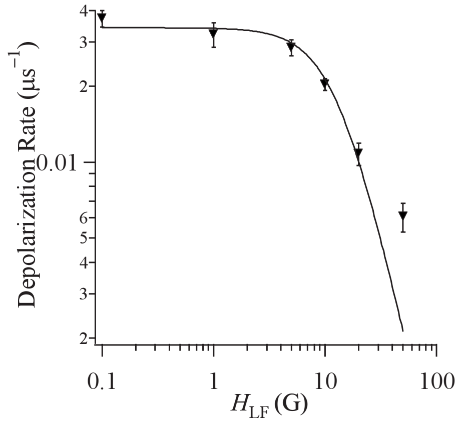

FIG. 6. Longitudinal-field dependence of the dynamic muon spin depolarization rate, λ_{CT}, for $(n\text{-}C_3H_7)_4N[Fe^{II}Fe^{III}(dto)_3]$ at 80 K in the cooling process. The solid line shows the best fit of Eq. (3).

$$\lambda_{CT}(H_{LF}) = \{\lambda_{0,n=3}(H_{LF}) - c_{n=3}\} - \{\lambda_{0,n=5}(H_{LF}) - c_{n=5}\}. \tag{2}$$

Here, $\lambda_{0,n=3}(H_{LF})$ and $\lambda_{0,n=5}(H_{LF})$ are the dynamic muon spin depolarization rates at the LF for $n=3$ and $n=5$, respectively. $c_{n=3}$ and $c_{n=5}$ are the mean values of the strong component of $\lambda_{0,n=3}(H_{LF})$ and $\lambda_{0,n=5}(H_{LF})$, respectively. The LF dependence of this subtracted depolarization rate λ_{CT} at 80 K is summarized in Fig. 6. The LF dependence of λ_{CT} shows a convex shape as a function of H_{LF} in a log-log plot and tends to disappear around 100 G. To obtain quantitative information on the dynamic properties of the electron transfer, the Redfield equation was applied. The Redfield equation[18,19] is expressed as

$$\lambda_{CT} = \frac{2\gamma_\mu^2 H_{loc}^2 \tau_C}{1 + \gamma_\mu^2 H_{LF}^2 \tau_C^2} \tag{3}$$

where τ_c and H_{loc} are the correlation time of muon spins and the amplitude of the fluctuating internal field at the muon site, respectively. The solid line in Fig. 6 is the best fit for Eq. (3). The same analysis was applied to the LF dependence of λ_{CT} measured at 60 and 110 K, and the calculated parameters are summarized in Table I. The frequency of the additional internal field at the muon site, which is given as $v = 1/\tau_c$, is on the order of 0.1 MHz as the maximum at 80 K and zero at 60 K. The magnitude of H_{loc} is from 2–4 G, which is larger than that of $\Delta(\sim 1\ \text{G})$.

TABLE I. Parameters obtained by fitting λ_{CT} for $(n\text{-}C_3H_7)_4N[Fe^{II}Fe^{III}(dto)_3]$ to Eq. (3).

T (K)	τ_C (μs)	H_{loc} (G)	$c_{n=3}$ (μs^{-1})
60		0	0.033
80	5.7	4.0	0.028
110	10.6	1.9	0.023

It can be suggested that the flip flop of a moving electron between Fe^{II} and Fe^{III} sites produces the dynamically fluctuating internal field at the muon site and its frequency is represented by υ. The time scale of τ_c is consistent with the result of the ^{57}Fe Mössbauer measurement, which implies that the fluctuation between the HTP and the LTP is slower than 10^{-7} s. It was reported that the resistivity of $n=3$ shows an anomalous drop with the thermal hysteresis loop within the temperature range of the CTPT.[20] Considering the present μSR results, it can be suggested that the hopping conduction in the $[Fe^{II}Fe^{III}(dto)_3]_\infty$ network is induced by the CTPT.

IV. SUMMARY

We have used a pulsed positive surface muon to probe the CTPT and the ferromagnetic phase transition of $(n\text{-}C_nH_{2n+1})_4N[Fe^{II}Fe^{III}(dto)_3]$ ($n=3$ and 5). In the case of $n=3$, an anomalous enhancement of the dynamic muon spin depolarization rate λ_0 was observed in ZF between 60 and 140 K. This anomalous enhancement is due to the dynamic oscillation of electron transfer between the Fe^{II} and Fe^{III} sites caused by the CTPT. The oscillation frequency, which was on the order of 0.1 MHz, was evaluated from the measurements of the LF dependence of the dynamic muon spin depolarization rate.

This is the first observation of the dynamic electron transfer process of such mixed-valence complexes by using the μSR technique. Therefore, μSR will open the initiating research on the dynamics of charge-transfer phenomena for various inorganic and organic charge-transfer complexes that exhibit CTPT or neutral-ionic phase transitions.

ACKNOWLEDGMENTS

The μSR measurements were supported by Toray Science and a Technology Grant and were also supported by the joint research project of the Japan Society for the Promotion of Science.

[1] T. Nakamoto, T. Miyazaki, M. Itoi, Y. Ono, N. Kojima, and M. Sorai, Angew. Chem., Int. Ed. **40**, 4716 (2001).

[2] N. Kojima, W. Aoki, M. Itoi, Y. Ono, M. Seto, Y. Kobayashi, and Yu. Maeda, Solid State Commun. **120**, 165 (2001).

[3] Y. Umezono, W. Fujita, and K. Awaga, J. Am. Chem. Soc. **128**, 1084 (2006).

[4] H. Tokoro, S. Ohkoshi, T. Matsuda, and K. Hashimoto, Inorg. Chem. **43**, 5231 (2004).

[5] N. Shimamoto, S. Ohkoshi, O. Sato, and K. Hashimoto, Inorg. Chem. **41**, 678 (2002).

[6] T. Mochida, K. Takazawa, M. Takahashi, M. Takeda, Y. Nishio, M. Sato, K. Kajita, H. Mori, M. M. Matsushita, and T. Sugawara, J. Phys. Soc. Jpn. **74**, 2214 (2005).

[7] M. Itoi, A. Taira, M. Enomoto, N. Matsushita, N. Kojima, Y. Kobayashi, K. Asai, K. Koyama, T. Nakano, Y. Uwatoko, and J. Yamaura, Solid State Commun. **130**, 415 (2004).

[8] N. Kojima, Y. Ono, K. Kobayashi, and M. Seto, Hyperfine Interact. **156/157**, 175 (2004).

[9] M. Itoi, Y. Ono, N. Kojima, K. Kato, K. Osaka, and M. Takata, Eur. J. Inorg. Chem. **6**, 1198 (2006).

[10] O. Berkooz, M. Mulamud, and S. Strikman, Solid State Commun. **6**, 185 (1968).

[11] C. T. Dziobkowski, J. T. Wrobleski, and D. B. Brown, Inorg. Chem. **20**, 679 (1981).

[12] R. D. Cannon, L. Montri, D. B. Brown, K. M. Marshall, and C. M. Elliott, J. Am. Chem. Soc. **106**, 2591 (1984).

[13] H. Sano, Hyperfine Interact. **53**, 97 (1990).

[14] K. Nagamine, T. Matsuzaki, K. Ishida, I. Watanabe, R. Kadono, G. H. Eaton, H. J. Jones, G. Thomas, and W. G. Williams, Hyperfine Interact. **87**, 1091 (1994).

[15] R. S. Hayano, Y. J. Uemura, J. Imazato, N. Nishida, T. Yamazaki, and R. Kubo, Phys. Rev. B **20**, 850 (1979).

[16] O. Hartmann, Hyperfine Interact. **49**, 61 (1989), and references cited therein.

[17] R. Kadono, T. Matsuzaki, T. Yamazaki, S. R. Kreitzman, and J. H. Brewer, Phys. Rev. B **42**, 6515 (1990).

[18] L. P. Le, A. Keren, M. I. Larkin, G. M. Luke, W. D. Wu, Y. J. Uemura, J. S. Miller, and A. J. Epstein, Phys. Rev. B **65**, 024432 (2001).

[19] W. Higemoto, H. Tanaka, I. Watanabe, and K. Nagamine, Phys. Lett. A **243**, 80 (1998).

[20] M. Enomoto, M. Itoi, Y. Ono, and N. Kojima, Synth. Met. **137**, 1231 (2003).